
Image denoising using fast non-local means filter and multi-thresholding with harmony search algorithm for WSN

H. Rekha* and P. Samundiswary

Department of Electronics Engineering,
School of Engineering and Technology,
Pondicherry University,
Pondicherry, India
Email: saathvekha16@gmail.com
Email: samundiswary_pdy@yahoo.com
*Corresponding author

Abstract: Several image denoising algorithms are developed so far to obtain a better denoised sensor images. But they fail to preserve the edges of the images. In order to overcome this, an attempt has been made in this paper by incorporating the various filters like fast non-local means filter (FNLMF) and high boost filter with the existing wavelet thresholding-based denoising method. However, the denoised output and the computation time are affected by the wavelet properties significantly. Hence, this paper concentrates on histogram-based multi-thresholding (HMT) as a major part to denoise the image. Here, the corrupted image is first denoised by applying FNLMF filtering section. Then the edges and minimal details of the denoised output are enhanced by utilising the HMT with harmony search algorithm (HSA)-based optimisation technique. From the simulation results, the proposed denoising method can be adoptable for WSN.

Keywords: bilateral filter; entropy; fast non-local means filter; histogram; image denoising; multi-thresholding; high boost filter; HBF; optimisation; harmony search algorithm; wavelet thresholding; wireless sensor network; WSN.

Reference to this paper should be made as follows: Rekha, H. and Samundiswary, P. (2023) 'Image denoising using fast non-local means filter and multi-thresholding with harmony search algorithm for WSN', *Int. J. Advanced Intelligence Paradigms*, Vol. 24, Nos. 1/2, pp.92–109.

Biographical notes: H. Rekha received her BE in Electronics and Communication Engineering from the Bharadidasan University, Tamilnadu, India in 2004 and MTech in Electronic and Communication from the Pondicherry Engineering College affiliated to Pondicherry University, Pondicherry, India in 2010. She is a student member of IET and IEICE. At present, she is pursuing her PhD in the Department of Electronics Engineering, Pondicherry University, Pondicherry, India. Her current research includes image processing and wireless multimedia sensor network.

P. Samundiswary received her BTech and MTech in Electronics and Communication Engineering from the Pondicherry Engineering College affiliated to Pondicherry University, Pondicherry, India in 1997 and 2003 respectively. She received her PhD from the Pondicherry Engineering College affiliated to Pondicherry University, Pondicherry, India in 2011. She has been

working in teaching profession since 1998. Currently, she is working as an Assistant Professor in the Department of Electronics Engineering, School of Engineering and Technology, Pondicherry Central University, India. She has nearly 18 years of teaching experience. She has published more than 90 papers in national and international conference proceedings and journals. She has co-authored a chapter of the book published by INTECH Publishers. She has been one of the authors of the book published by LAMBERT Academic Publishing. Her area of interest includes wireless communication and networks, wireless security and computer networks.

This paper is a revised and expanded version of a paper entitled 'Image denoising using hybrid of bilateral filter and histogram based multi-thresholding with optimization technique for WSN' presented at International Conference on Advances in Computational Intelligence and Communication (CIC 2016), Pondicherry Engineering College, Puducherry, India, 19 and 20 October 2016.

1 Introduction

Due to the recent advancements of wireless sensor network (WSN), it is chosen as the best networking technology for many applications including object tracking, telemedicine and forest monitoring etc. The main advantage of using WSN is that, it is infrastructure less and low cost. Despite the advantages of WSN, it has very limited power, less storage space and low coverage area. Besides, noise is considered as a major factor affecting the WSN during image acquisition, transmission and reception. From the various literature studies (McVeigh et al., 1985; Gonzalez and Woods, 2002; Marpe et al., 2002), it is understood that, there are several types of noises corrupting the images during the transmission and reception of images through WSNs. Basically the noises occurred in the image-based applications are categorised in terms of their density level with respect to the atmospheric condition and the quality of cameras used (Buades et al., 2005). Some of the practical noises that frequently trouble the images are additive white Gaussian noise (AWGN), salt and pepper noise, shot noise, etc. Out of these kind of practical noises, the AWGN noise during image acquisition produce severe problems than that of other practical noises. Until now, there are lots of researches prevailing in image denoising techniques to find the best solution for suppressing the impact of AWGN noise density level over image. But the trade off between the computational cost and the amount of noise suppression is yet to be a complicated problem. In particular, for example, the transform-based techniques so far used (Wenxuan et al., 2010; Khare and Tiwary, 2007; Ghazel, 2004) are succeeded to reduce the noise level with better image quality at the cost of high energy consumption.

For the past two decades, spatial-based techniques (Mitiche et al., 2013; Roy et al., 2010; da Silva et al., 2013; Srinivasan and Ebenezer, 2007) have provided better improvements in the field of denoising techniques to reduce the computation cost. However, there is a trade-off between the image quality and computational complexity. A number of approaches have been developed based on spatial-based image denoising methods to reduce the computation complexity significantly. Shreyamsha Kumar (2013) has combined the spatial filter called Gaussian/bilateral filter (GBF) with the wavelet

thresholding (WT) to improve the quality of the denoised image. Naimi et al. (2015) have embedded the wiener filter with the WT (discrete wavelet transform) in order to recover the fine details from the noisy medical images. These techniques can perform well to a certain extent and cause artefacts for higher noise level variations because of the wavelet properties.

There are several wavelet-based denoising methods used to reduce the gaussian noise during image pre-processing. Out of that, WT and its combination with the bilateral filter (BF) have shown better results in terms of quantitatively and qualitatively. But, for higher noise levels, the denoised images of BF and its updated version called fast bilateral filter (FBF) are poorly affected by over smoothing and blurring. In the meantime, several researchers have focused on different meta-heuristic optimisation algorithms. Toledo et al. (2013) have made an attempt to incorporate them in many image processing applications in order to reduce the searching period as well to find the optimal solution. Later, de Paiva et al. (2015) have tried to hybridise one of the optimisation algorithms called genetic algorithm with three different denoising methods such as block matching and 3D filtering (BM3D) (Dabov et al., 2006), wiener-chop (Ghael et al., 1997) and anisotropic diffusion (Black et al., 1998) to improve the denoising quality with less complexity. After that, Chandra and Chattopadhyay (2014) have designed an image denoising algorithm using low pass filter along with the incorporation of the differential evolution (DE)-based optimisation method. Here the DE is used to evaluate the fittest optimal filter coefficients. Later, Bhandari et al. (2015) has modified the wavelet-based adaptive thresholding technique by using the DE algorithm to eradicate the problems like edge smoothening and blurring.

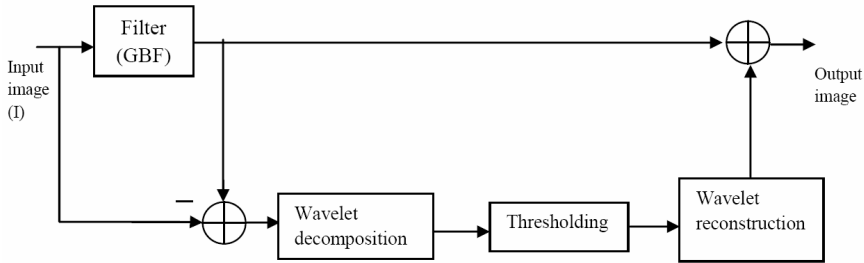
Recently, Rekha and Samundiswary (2016) have tried an attempt on sensor images by combining the BF and histogram-based multi-thresholding (HMT) using harmony search algorithm. However, this method is not adaptable for high noise levels. Hence, in this paper the proposed method first considers the several image filters such as Wiener Filter (WF), fast non-local means filter (FNLMF), FBF and high boost filter (HBF) along with the existing WT technique and tested for various standard noisy images. After the careful evaluation of the different image filters, the FBF and FNLMF-based denoising methods provide better results in terms of image quality and performance metrics such as peak signal to noise ratio (PSNR), image quality index (IQI), and normalised absolute error (NAE). But the computation time and complexity of the algorithm is more and not applicable for WSN. Hence, to reduce the computation time further, the proposed method concentrates on two image filters called FBF and FNLMF with the combination of HMT with Shannon entropy and HSA-based optimisation technique for effective AWGN noise reduction. In the proposed method, the low frequency noise is partially eliminated by using a denoising filter, then the fine details of the input image is enhanced by using HMT with optimisation.

The rest of the paper is organised as follows: Section 2 deals with the brief description about the existing image denoising method with WT technique. Section 3 explains about the basic concepts of the HMT and FNLMF. Section 4 discusses about the working principle of the proposed denoising algorithm with image compression and optimisation technique with the help of a neat diagram. Section 5 deals with the simulation results and discussion about the proposed method with the existing WT methods in terms of their performance metrics like PSNR, IQI and computation time. Finally, Section 6 concludes the proposed work based upon the result analysis, and the future work is also discussed in Section 6.

2 Existing image denoising technique

Recently, Shreyamsha Kumar (2013) has proposed an image denoising algorithm based on GBF with WT. In this technique, the author has considered the WT as a major part to improve the denoised image features and to avoid the loss of image details and edge smoothing due to the effect of BF.

Figure 1 Block diagram of the existing image denoising algorithm using GBF and WT



The working principle of the existing model is illustrated in Figure 1. Here the Gaussian noise corrupted input image is first fed into the filtering section to reduce the noise level by replacing the pixels into its average weights. Then the difference between the noisy input image and the filter output image is applied into the wavelet block for thresholding. Here, the noisy image is decomposed into low frequency components depending upon the number of decomposition level. Followed by the wavelet, the decomposed wavelet coefficients are sent in to the bayeshrink model for perfect thresholding of decomposed coefficients. Finally, the quality of the denoised image is improved by adding the enhanced version of wavelet threshold output with the smoothed output of the filter. Generally, the difference between the input image and its noise free output image shows the impact of the denoising method over noisy images. However, at high noise levels, the performance of the WT output is not appreciable for images with more number of features.

3 Methodologies used for the proposed algorithm

The following two methods are used as major blocks for constructing the proposed image denoising algorithm.

3.1 Fast non-local means filter

Non-local means filter algorithms are mainly used for images which contains many repetitive structured patterns. It reduces the redundant features by performing a weighted average of pixel values to reduce the amount of noise present in the image. Formally, consider the images defined over a discrete regular grid Ω of dimension d and cardinality $|\Omega|$. By assuming 'v' as the original noisy image, then the restored image 'u' can be calculated at a site $s \in \Omega$

$$u(s) = \frac{1}{Z(s)} \sum_{t \in N(s)} w(s, t)v(t) \tag{1}$$

where $w(s, t)$ are non-negative weights, $Z(s)$ is called as normalisation constant and $N(s)$ corresponds to a set of neighbouring sites of s . The searching window is referred as $N(\cdot)$. The similarity between two square patches is measured by using a weight $w(s, t)$ respectively at sites s and t , and it is defined as follows

$$w(s, t) = gh \left(\sum_{\delta \in \Delta} G_{\sigma}(\delta)(v(s + \delta) - v(t + \delta))^2 \right) \tag{2}$$

where G_{σ} is a Gaussian kernel of variance σ^2 , $gh : IR^+ \rightarrow IR^+$ is a continuous non-increasing function with $gh(0) = 1$ and $\lim_{x \rightarrow +\infty} gh(x) = 0$, and $\Delta(\Delta = [-p, p])$ denotes the discrete patch region containing the neighbouring sites δ . The usage of parameter h is to control the amount of filtering. In general, by taking into account spatial values and intensity similarities between pixels, non-local (NL) means to restore the image features by performing a weighted average of pixel values. In this, similarity is computed between equally sized patches as they capture the local structures (geometry and texture) around the sites in consideration. It is important to note that pixels outside $N(s)$ do not contribute to the value of $u(s)$. This property allows the image to separate into independent disjoint pieces and processes them in parallel, which is done in domain decomposition models.

As from equation (2), the weight computation $w(s, t)$ is one of the time consuming parts when generating the restored image u . This is avoided by replacing the Gaussian kernel by the constant without noticeable differences. The modified weight equation is given below

$$w(s, t) = gh(sd_x(s + p) - sd_x(s - p)) \tag{3}$$

where sd_x is related to the discrete integration of the squared difference of the image ‘ v ’ and its translation vector d_x . The sd_x is given below

$$sd_x(p) = \sum_{k=0}^p (v(k) - v(k + d_x))^2, \quad p \in \Omega \tag{4}$$

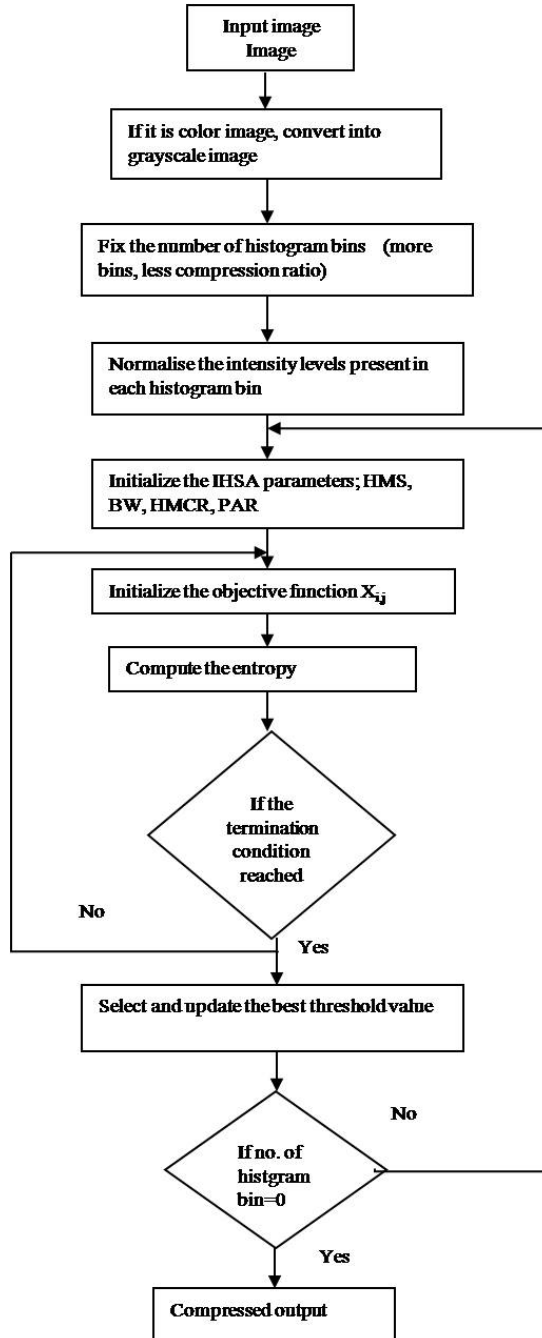
The quality of the FNLMF is improved than that of the existing FNLMF by using the above mentioned weighted computation. But, if the noise level increases to a certain level, then the sharpness of the image edges are not appreciable. Hence, to enhance the quality of the denoised image, additional block is needed which is explained in the following section.

3.2 *Histogram-based multi-level image thresholding with harmony search algorithm*

The most popular global thresholding schemes used in image processing are hard thresholding and soft thresholding. The choice of thresholding mainly depends upon the type of application. The major problem with both thresholding methods is the selection of the suitable threshold. There are lot of researches going on to find the appropriate threshold for concerned noisy images. This led to the idea of a non-uniform thresholding which uses different thresholds for different noise levels. But, this type of thresholding

produces smoothed edges and reduces the sharpness of the denoised image. Hence, Pun (1980) has introduced another method called histogram-based multi-level thresholding for global multi-thresholding.

Figure 2 Flowchart of the working model of HSA-based HMT



In that method, the noisy input image is first separated into several objects by analysing the profile characteristics of the image histogram or by optimising a certain objective function. Then the threshold value of each object is calculated by using the entropy. There are different entropy-based methods (Albuquerque et al., 2004; Benzid et al., 2008; Sahoo and Arora, 2004) which have been proposed for multi-level thresholding. In particular, the performance of the HMT technique mainly depends upon the selection of number of thresholds and the entropy. Once the number of threshold values is chosen, the image is first separated into number of histogram bins. Then the histogram is approximated by using the maximisation of Shannon's entropy. If the numbers of thresholds is high, the denoising process becomes complicated and it increases the computational time almost exponentially. Because of this reason, an optimisation algorithm called harmony search algorithm is incorporated with the HMT concept.

Before applying the HSA in to the multi-thresholding algorithm, the parameters such as harmony memory (HM), harmony memory consideration rate (HMCR), pitch adjusting rate (PAR) and BandWidth (BW) should be fixed (Mahdavi et al., 2007) with suitable values in order to achieve better performance. Determining and fixing the most appropriate values to the parameters for a particular analysis is not an easy task, since such parameters interact to each other in a highly nonlinear manner. Also there is no proper mathematical model available for the above mentioned interaction. Hence, the common method to find the best set of parameter values is done by using a random number within the parameter value limits and then the optimisation algorithm HSA is executed. If the final optimum value is not satisfactory; then a new set of parameter values is created and the optimisation algorithm is executed again. The basic working principle of HSA-based HMT is clearly depicted by using the flowchart as shown in Figure 2 and also it is well explained with the help of mathematical expressions as given below.

As per the multi-thresholding concept, the input image is first segmented into number of histogram bins. Let L grey levels are to be assumed in a given image I and the grey levels are splitted into $0, 1, 2, \dots, L-1$, the range of each bin to calculate the threshold value (H) are obtained by using the following equation (5) to equation (8)

$$H_0 = \{(x, y) \in I \mid 0 \leq f(x, y) \leq t_1 - 1\} \quad (5)$$

$$H_1 = \{(x, y) \in I \mid t_1 \leq f(x, y) \leq t_2 - 1\} \quad (6)$$

$$H_2 = \{(x, y) \in I \mid t_2 \leq f(x, y) \leq t_3 - 1\} \quad (7)$$

$$H_k = \{(x, y) \in I \mid t_k \leq f(x, y) \leq L - 1\} \quad (8)$$

where $f(x, y)$ is the grey level of the point (x, y) , $t_i (i = 1, 2 \dots k)$ is the i^{th} threshold value and k is the number of the thresholds. The selection of the optimal threshold using bi-level thresholding is not a complex issue. But, the selection of more than few optimal threshold values for multi-level thresholding requires a high computational cost. In order to find the appropriate threshold values (H), the entropy concept is utilised. The entropies of each group of grey levels are

$$\begin{aligned}
 H_1 &= -\sum_{i=0}^{T_1} \frac{p_i}{p_1} \ln \frac{p_i}{p_1}, \\
 H_2 &= -\sum_{i=T_1+1}^{T_2} \frac{p_i}{p_2} \ln \frac{p_i}{p_2} \dots\dots\dots, H_{n+1} = -\sum_{i=T_n+1}^{L-1} \frac{p_i}{p_n} \ln \frac{p_i}{p_n}
 \end{aligned}
 \tag{9}$$

where the probability of occurrence (p) can be calculated by using

$$p_1 = \sum_{i=0}^{T_1} h_i, p_2 = \sum_{i=T_1+1}^{T_2} h_i, \dots\dots\dots, p_{n+1} = \sum_{i=T_n+1}^{L-1} h_i$$

Then the total entropy will be

$$H(T) = H_1 + H_2 + \dots\dots\dots + H_{n+1}
 \tag{10}$$

For effective multi-thresholding, the best optimal thresholds (T^*) can be obtained by maximising the total entropy using HSA optimisation technique.

$$T^* = \max(H(T))
 \tag{11}$$

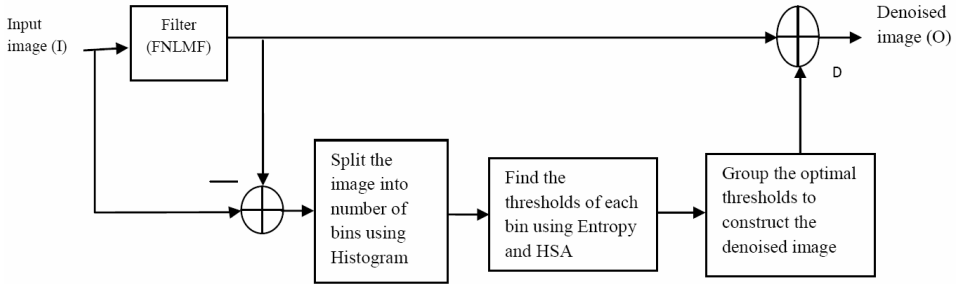
Actually, the selection of the optimal threshold value is done after a several improvisations of HSA. Once the iteration is started, the harmony search algorithm updates the HM value by comparing the recent solution with the worst solution. At the end of the iteration, the optimisation algorithm finds the best optimal threshold value of the particular histogram bin. The above concept is repeated for each histogram bin to find the best optimal thresholds. Finally, the optimal thresholds from each histogram bin are used to reconstruct the resultant histogram image with fine detail.

4 Proposed image denoising method

To enhance the quality of the performance metrics and to reduce the computational complexity of the existing WT-based image denoising algorithm, the proposed algorithm replaces the WT by histogram-based multi-thresholding. The working model of the proposed image denoising algorithm is shown in Figure 3. The selection of the filter method for initial denoising mainly depends upon the quality and sharpness of the image details. In that case FNLMF is superior to that of the bilateral filtering and other existing denoising filters. But, from the literature survey, the denoised output of the FNLMF is lacking in preserving the image edges. Hence, in the proposed denoising method, the noisy input image is fed parallel into the FNLMF as well as to HMT block. Then, the summation of the two output images such as FNLMF output and HMT output produces the denoised image with better image quality. The usage of multi-thresholding in the proposed method is to improve the sharpness of image edges and reduce the noise level over image. Generally, the selection of more number of thresholds for multi-thresholding will gradually increase the complexity of the algorithm. Also, the calculation of threshold value using entropy is not accurate to reconstruct the denoised output image. Hence, to reduce the computation time and to find the optimal threshold value, the optimisation algorithm is utilised. From the literature review (Mahdavi et al., 2007; Oliva et al., 2013), the performance of the HSA is better than that of the other optimisation algorithms in

terms of simplicity and fast convergence. Due to this, the HSA-based optimisation is taken into consideration for the proposed denoising method.

Figure 3 Proposed image denoising model using histogram-based multi-thresholding and HAS



In Figure 3, the usage of the FNLMF over the noisy image averages the noise along with the image details while preserving the edges. Then the difference between the noisy image and the filter output is fed into the HSA-based multi-thresholding section. The difference image which is having only low frequency details is separated into number of bins. Then, by using Shannon entropy and HSA, the optimal thresholds are selected and the variation in the pixel values over noisy image is reduced. The main contribution of HSA in multi-thresholding is to reduce the computational complexity and for maximising the entropy output. Further, the resultant histogram image from HSA-based multi-thresholding is added with the FNLMF output to get the better denoised output image. The output image provides better image quality than that of the existing techniques. It is noted that, the quality of the denoised image is retained for a certain noise level only. For, e.g., if the noise level increases beyond 50%, then the loss of image detail will be unavoidable.

5 Result and discussion

To understand the effectiveness of the FNLMF in proposed image denoising algorithm with optimisation technique, the original images are first corrupted by a AWGN noise with zero mean and different noise deviations [$\sigma \in 10, 20, 30, 40$] respectively. For analysing the robustness of the proposed algorithm, various benchmark images with different sizes are considered and few images from UC Berkley dataset are also taken into account in this paper as shown in Figure 4.

Lena grayscale image is considered as the first image with the size of 512×512 . Next, the cameraman and baboon image, both having the same size of 256×256 and another is a sensor image of size 481×382 taken from image dataset of UC Berkley, which is popular for sensor images. To investigate the efficiency of the proposed method over noisy images, the commonly used performance metrics such as PSNR, IQI and computation time are examined. These parameter values are used to verify the reliability and the overall quality of the denoised output image. The simulation parameters of the optimisation algorithm and the filters with their values are listed in Table 1.

Figure 4 Standard input images considered for simulation, (a) Lena image (b) cameraman image (c) Baboon image (d) sensor image

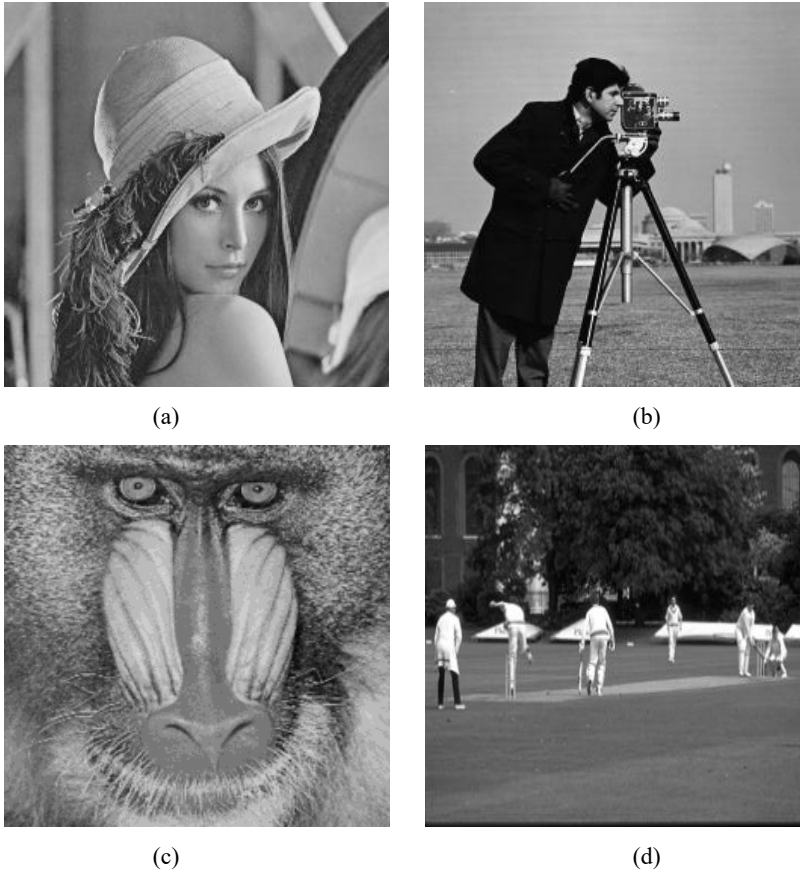


Table 1 Simulation parameters

<i>Parameter</i>	<i>Value</i>
For HSA	
Harmony memory size	100
Pitch adjusting rate	0.9
H MCR	0.95
BandWidth	[0, 1]
No. of thresholds	60
For BF	
Window size	11×11
Spatial width (σ_s)	1.8
Range width (σ_r)	40
For FNLMF	
Patch radius (f)	10
Searching range (t)	2

5.1 Quantitative analysis

In order to improve the effectiveness of the existing WT-based denoising, three classic filters namely WF, FNLMF and HBF are exploited. Then the proposed HMT-based denoising algorithm with Shannon entropy and HSA is compared with the WT-based denoising algorithm with different filter combinations of various noise deviations. Tables 2, 3, 4 and 5 shows the PSNR and IQI results of the existing and the proposed denoising methods with the consideration of the corrupted input images. It is noted from all the tables that the first five methods depict the results of the existing WT-based denoising methods and the last two are the proposed HMT-based denoising methods. The first and the second method reported are based on the BF and FBF. The third method is the wiener filter combination. To check the effect of enhancement filter in the denoising method, the fourth method considers a HBF. Moreover, FNLMF is considered as a fifth method. The proposed denoising method using FNLMF and FBF filters are shown as the sixth and the seventh method in the table.

Table 2 Performance comparison of Lena image for various noise levels using different denoising methods

Image	Filter	Noise deviation		$\sigma = 10$		$\sigma = 20$		$\sigma = 30$		$\sigma = 40$		
		PSNR	IQI	PSNR	IQI	PSNR	IQI	PSNR	IQI			
LENA	GBF+WT (B.K. Shreyamsha Kumar, 2013)	31.79	0.991	28.15	0.980	26.28	0.975	25.15	0.965			
	FBF+WT	31.77	0.991	28.00	0.981	26.08	0.970	24.93	0.963			
	WF+WT	31.76	0.991	28.37	0.982	26.48	0.973	24.82	0.962			
	HBF+WT	31.04	0.989	27.48	0.979	25.89	0.972	24.72	0.963			
	FNLMF+WT	32.42	0.992	29.41	0.985	27.26	0.976	25.66	0.966			
	Proposed HMT-based image denoising with HSA optimisation and Shannon entropy											
	FBF+HMT+HSA	31.43	0.990	28.22	0.977	26.47	0.967	25.26	0.960			
FNLMF+HMT+HSA	32.52	0.992	29.60	0.982	27.61	0.978	26.16	0.964				

Table 3 Performance comparison of cameraman image for various noise levels using different denoising methods

Image	Filter	Noise deviation		$\sigma = 10$		$\sigma = 20$		$\sigma = 30$		$\sigma = 40$		
		PSNR	IQI	PSNR	IQI	PSNR	IQI	PSNR	IQI			
Cameraman	GBF+WT (B.K. Shreyamsha Kumar, 2013)	31.89	0.991	27.84	0.981	25.51	0.971	23.87	0.963			
	FBF+WT	31.89	0.991	27.79	0.981	25.34	0.970	23.75	0.961			
	WF+WT	30.52	0.984	27.73	0.979	25.79	0.972	24.03	0.964			
	HBF+WT	31.15	0.991	27.07	0.979	24.94	0.969	23.53	0.960			
	FNLMF+WT	31.55	0.990	28.77	0.983	26.72	0.974	24.86	0.966			
	Proposed HMT-based image denoising with HSA optimisation and Shannon entropy											
	FBF+HMT+HSA	31.50	0.994	28.08	0.983	25.41	0.974	23.64	0.960			
FNLMF+HMT+HSA	31.75	0.991	28.86	0.987	26.78	0.975	24.94	0.969				

Table 4 Performance comparison of Baboon image for various noise levels using different denoising methods

Image	Filter	Noise deviation		$\sigma = 10$		$\sigma = 20$		$\sigma = 30$		$\sigma = 40$		
		PSNR	IQI	PSNR	IQI	PSNR	IQI	PSNR	IQI			
Baboon	GBF+WT (B.K. Shreyamsha Kumar, 2013)	32.02	0.988	28.02	0.973	25.82	0.956	24.40	0.942			
	FBF+WT	32.01	0.988	28.10	0.972	25.80	0.955	24.31	0.941			
	WF+WT	30.44	0.981	27.62	0.968	25.62	0.955	24.25	0.941			
	HBF+WT	31.76	0.987	27.81	0.971	25.73	0.956	24.34	0.941			
	FNLMF+WT	31.90	0.988	28.12	0.973	25.88	0.956	24.42	0.941			
	Proposed HMT-based image denoising with HSA optimisation and Shannon entropy											
	FBF+HMT+HSA	29.98	0.974	26.05	0.944	24.73	0.923	23.85	0.907			
FNLMF+HMT+HSA	32.46	0.989	28.14	0.979	25.83	0.956	24.59	0.951				

Table 5 Performance comparison of sensor image for various noise levels using different denoising methods

Image	Filter	Noise deviation		$\sigma = 10$		$\sigma = 20$		$\sigma = 30$		$\sigma = 40$		
		PSNR	IQI	PSNR	IQI	PSNR	IQI	PSNR	IQI			
Sensor image	GBF+WT (B.K. Shreyamsha Kumar, 2013)	31.49	1.0	27.67	0.989	25.47	0.966	24.07	0.957			
	FBF+WT	31.49	0.992	27.67	0.974	25.44	0.967	24.05	0.952			
	WF+WT	30.82	0.990	28.05	0.987	26.13	0.966	24.34	0.960			
	HBF+WT	30.97	0.999	27.23	0.997	25.20	0.951	23.90	0.952			
	FNLMF+WT	31.03	0.991	28.32	0.982	26.37	0.972	24.79	0.961			
	Proposed HMT-based image denoising with HSA optimisation and Shannon entropy											
	FBF+HMT+HSA	30.79	0.989	27.83	0.979	25.90	0.967	24.41	0.952			
FNLMF+HMT+HSA	30.82	0.991	28.43	0.989	26.45	0.974	25.05	0.960				

It is inferred through the *PSNR* results of the different images, that the denoised output of HBF with WT is found to be good at low noise deviations ($\sigma = 10$ and 20) but it is having poor *PSNR* for high noise deviations of 30 and 40 . Further, the wiener filter also provides better *PSNR* for standard Lena and cameraman image for higher noise deviations of 30 and 40 . But for the Baboon and sensor image, it shows no improvement. Due to this, the HBF and WF is not applicable for practical WSN-based applications. In many cases, the GBF and FBF with WT are having the acceptable *PSNR* and *IQI* values. However at $\sigma = 40$, the *PSNR* and *IQI* values of denoising method using above mentioned filters are not appreciable compared to that of the FNLMF results. For example, if Lena, cameraman and sensor image are considered as input images, then the *PSNR* value of the FNLMF is 1 dB superior to that of the BF.

It is inferred through the results of the proposed method (filter + HMT) using HSA optimisation shown in Tables 2, 3, 4 and 5, that the key factor used to determine the performance of the proposed method is the selection of thresholds and optimisation algorithm. To reduce the computational complexity of the algorithm, the number of

thresholds is fixed as 60. From the proposed method (using FBF+ HMT and FNLMF+ HMT), there is not much difference in PSNR and IQI values for Cameraman and sensor image. But there is a huge difference for the Lena and Baboon image, i.e., the performance metrics of the proposed FNLMF with HMT is far better than that of the proposed FBF with HMT.

Table 6 Average computation time of different denoising methods for various images

<i>Filter/image</i>	<i>Average computation time (sec)</i>			
	<i>Lena</i>	<i>Cameraman</i>	<i>Mandrill</i>	<i>Sensor</i>
GBF+WT (B.K.Shreyamsha Kumar, 2013)	3.25	3.40	11.21	7.125
FBF+WT	1.167	1.266	2.734	1.72
WF+WT	0.823	0.95	1.17	0.966
HBF+WT	0.957	1.06	1.986	1.356
FNLMF+WT	1.231	1.257	2.65	1.97
Proposed HMT-based image Denoising with HSA optimisation and Shannon entropy				
FBF+HMT+HSA	2.13	1.95	2.973	6.38
FNLMF+HMT+HSA	1.08	1.11	2.21	1.52

The real-time performance of the denoising algorithm to be used for WSN mainly depends on their computation time. Hence, the computation time is taken as a primary selection criterion for the selection of better image denoising method. In Table 6, the computation time of the proposed HMT-based denoising method with two different filters such as FBF and FNLMF is compared with the existing WT technique with different filter combinations. It is observed from the table that the overall running time of the WT with the WF and HBF are very less compared to that of the other denoising algorithms. But they show very poor performance for higher noise standard deviations. So they are not considered for further comparison.

It is portrayed through the results of the proposed method listed in Table 6 that the average running time of the FBF is one fold higher than that of the FNLMF which means the combination of FNLMF +HMT with HSA-based optimisation is having less computation time. Also from Tables 2, 3, 4 and 5, it is concluded that the overall performance of the proposed HMT with HSA-based optimisation along with the combination of FNLMF is more appropriate for WSN.

5.2 Qualitative analysis

Generally, the estimation of the PSNR is not enough to judge the visual quality of the denoised image. Therefore, visual inspections are also necessary to measure the amount of preservation of edge details and the artefacts. For demonstration purpose, two images are taken as test sample for visual evolution of all denoising methods.

Figure 5 Qualitative analysis of Lena image using different denoising method for various noise levels

























































Filter	$\sigma = 10$	$\sigma = 20$	$\sigma = 30$	$\sigma = 40$
BF+WT				
WF+WT				
FBF+WT				
FNLMF+WT				
HBF+WT				
Proposed FBF+HMT+HSA				
Proposed FNLMF+HMT+HSA				

Figure 6 Qualitative analysis of the sensor image using different denoising methods for various noise levels

Filter	$\sigma = 10$	$\sigma = 20$	$\sigma = 30$	$\sigma = 40$
BF+WT				
WF+WT				
FBF+WT				
FNLMF+WT				
HBF+WT				
Proposed FBF+HMT+HSA				
Proposed FNLMF+HMT+HAS				

It is observed from Figure 5 that, the denoised output of the proposed method using FNLMF with HMT provides more details near the eyes and hat portion of the Lena

image. Also it is having a sharp edge details compared to that of FBF at high noise deviation ($\sigma = 30, 40$). But the WT-based image denoising with different filter combinations for $\sigma = 30$ and 40 does not achieve good image quality because of edge smoothening and blurring effect. It is also observed from the sensor image as shown in Figure 6, the performance of the BF and the HBF with WT is better and they are showing less blurring for noise deviations of 10 and 20 . If the noise level increases more than 20 , it fails to recover the background features of the denoised image. But in the proposed method, the impact of HMT helps to preserve the background details at high noise levels. From the visual perception, the thresholding technique HMT with the combination of FNLMF produces better image quality for all noise standard deviations.

Overall, the combination of the FNLMF and HMT with Shannon entropy and harmony search optimisation algorithm achieves better results in reduction of Gaussian noise compared to that of the other techniques. Both the qualitative and quantitative analysis indicate that the combination of FNLMF filter and HMT with HSA-based optimisation algorithm effectively suppresses the noise with less degradation of image details even at higher noise level.

6 Conclusions

In this paper, the image filters FBF and FLMF with the combination of HMT using harmony search algorithm is proposed as a major part to denoise the image. The excellent features such as selection of the optimal threshold and less computation time of the multi-thresholding with optimisation make it more suitable for image denoising. The performance of the proposed technique is compared with the existing WT method using different filter combinations. The filters taken for comparison are wiener filter, HBF, BF and FNLMF respectively. From the simulation results, it is understood that the integration of the FNLMF and HMT with Shannon and HSA achieves better results in terms of preserving the edges and quantitative parameter values (PSNR and IQI) than that of other existing denoising methods. Also the proposed algorithm provides less computation time for processing the various images for different noise levels. Thus it can be used as a pre processing stage for image-based wireless sensor applications. In the future work, different optimisation combinations can be incorporated in the proposed method and tested with the real time sensor images in order to improve the performance under various noise deviations values.

References

- Albuquerquea, M.P., Esquefb, I.A. and Melloa, A.R.G. (2004) 'Image thresholding using Tsallis entropy', *Pattern Recognition Letters*, Vol. 25, No. 9, pp.1059–1065.
- Benzid, R., Arar, D. and Bentoumi, M. (2008) 'A fast technique for gray level image thresholding and quantization based on the entropy maximization', *Proceedings of 4th International Conference on Swarm, Evolutionary and Memetic Computing*, Chennai, India, pp.1–4.
- Bhandari, A.K., Kumar, D., Kumar, A. and Singh, G.K. (2015) 'Optimal sub-band adaptive thresholding based edge preserved satellite image denoising using adaptive differential evolution algorithm', *Neurocomputing*, Vol. 174, Part B, pp.698–721.
- Black, M.J., Sapiro, G., Marimont, D.H. and Heeger, D. (1998) 'Robust anisotropic diffusion', *IEEE Transactions on Image Processing*, Vol. 7, No. 3, pp.421–432.

- Buades, A., Coll, B. and Morel, J.M. (2005) 'A review of image denoising methods, with a new one', *Multiscale Modelling and Simulation*, Vol. 4, No. 2, pp.490–530.
- Chandra, A. and Chattopadhyay, S. (2014) 'A new strategy of image denoising using multiplier-less FIR filter designed with the aid of differential evolution algorithm', *Multimedia Tools and Applications*, Vol. 75, No. 2, pp.1079–1098.
- da Silva, R.D., Minetto, R., Schwartz, W.R. and Pedrini, H. (2013) 'Adaptive edge-preserving image denoising using wavelet transforms', *Pattern Analysis and Applications*, Vol. 16, No. 4, pp.567–580.
- Dabov, K., Foi, A., Katkovnik, V. and Egiazarian, K. (2006) 'Image denoising with block-matching and 3D filtering', *SPIE Electronic Imaging: Algorithms and Systems*, Vol. 6064, No. 6064A-30, pp.1–14.
- de Paiva, J.L., Toledo, C.F.M. and Pedrini, H. (2015) 'An approach based on hybrid genetic algorithm applied to image denoising problem', *Applied Soft Computing*, Vol. 46, No. 1, pp.778–791.
- Ghael, S., Ghael, E.P., Sayeed, A.M. and Baraniuk, R.G. (1997) 'Improved wavelet denoising via empirical wiener filtering', *Proceedings of SPIE Wavelet Applications in Signal and Image Processing*, San Diego, CA, USA, Vol. 3169, pp.389–399.
- Ghazel, M. (2004) *Adaptive Fractal and Wavelet Image Denoising*, PhD thesis, Department of Electrical and Computer Engineering, University of Waterloo, Ontario, Canada.
- Gonzalez, R.C. and Woods, R.E. (2002) *Digital Image Processing*, 2nd ed., Prentice-Hall, Englewood Cliffs, New Jersey.
- Khare, A. and Tiwary, U.S. (2007) 'Daubechies complex wavelet transform based technique for denoising of medical images', *International Journal of Image and Graphics*, Vol. 7, No. 4, pp.663–687.
- Mahdavi, M., Fesanghary, M. and Damangir, E. (2007) 'An improved harmony search algorithm for solving optimization problems', *Journal of Applied Mathematics and Computation*, Vol. 188, No. 2, pp.1567–1579.
- Marpe, D., Cycon, H.L., Zander, G. and Barthel, K-U. (2002) 'Context-based denoising of images using iterative wavelet thresholding', *Proceedings of SPIE on Visual Communications and Image Processing*, San Jose USA, Vol. 4671, pp.907–914.
- McVeigh, E.R., Henkelman, R.M. and Bronskill, M.J. (1985) 'Noise and filtration in magnetic resonance imaging', *Medical Physics*, Vol. 12, No. 5, pp.586–591.
- Mitiche, L., Adamon-Mitiche, A.B.H. and Naimi, H. (2013) 'Medical image denoising using dual tree complex thresholding wavelet transform', *Proceedings of IEEE conference on Applied Electrical and Computing Technologies*, Jordon, pp.1–5.
- Naimi, H., Adamou-Mitiche, A.B.H. and Mitiche, L. (2015) 'Medical image denoising using dual tree complex thresholding wavelet transform and wiener filter', *Journal of King Saud University – Computer and Information Sciences*, Vol. 27, No. 1, pp.40–45.
- Oliva, D., Cuevas, E., Pajares, G., Zaldivar, D. and Perez-Cisneros, M. (2013) 'Multilevel thresholding segmentation based on harmony search optimization', *Journal of Applied Mathematics*, No. 1, pp.1–24.
- Pun, T. (1980) 'A new method for gray-level picture thresholding using the entropy of the histogram', *Signal Processing*, Vol. 2, No. 3, pp.223–237.
- Rekha, H. and Samundiswary, P. (2016) 'Image denoising using hybrid of bilateral filter and histogram multi-thresholding with optimization technique for WSN', *Special Issue – International Journal of Computer Science and Information Security*, Vol. 14, No. 1, pp.29–35.
- Roy, S., Sinha, N. and Sen, A.K. (2010) 'A new hybrid image denoising method', *International Journal of Information Technology and Knowledge Management*, Vol. 2, No. 2, pp.491–497.
- Sahoo, P.K. and Arora, G. (2004) 'A thresholding method based on two dimensional Renyi's entropy', *Pattern Recognition*, Vol. 37, No. 6, pp.1149–1161.

- Shreyamsha Kumar, B.K. (2013) 'Image denoising based on Gaussian/bilateral filter and its method noise thresholding', *Signal Image and Video Processing*, Vol. 7, No. 6, pp.1159–1172.
- Srinivasan, K.S. and Ebenezer, D. (2007) 'A new fast and efficient decision-based algorithm for removal of high-density impulse noises', *IEEE Signal Processing Letters*, Vol. 14, No. 4, pp.189–192.
- The Berkley Segmentation Dataset and Benchmark (BSDS500) [online]
<https://www2.eecs.berkeley.edu/Research/Projects/CS/vision/bsds/> (accessed 24 September 2016).
- Toledo, C., de Oliveira, L., Dutra da Silva, R. and Pedrini, H. (2013) 'Image denoising based on genetic algorithm', *IEEE Congress on Evolutionary Computation*, pp.1294–1301.
- Wenxuan, S., Jie, L. and Minyuan, W. (2010) 'An image denoising method based on multiscale wavelet thresholding and bilateral filtering', *Wuhan University Journal of Natural Sciences*, Vol. 15, No. 2, pp.148–152.